UNDERWATER COMMUNICATION THROUGHT MAGNETIC INDUCTION (MI)

by

Sana Ramadan

Submitted in partial fulfilment of the requirements
for the degree of Master of Applied Science

at

Dalhousie University
Halifax, Nova Scotia
October 2017

TABLE OF CONTENTS

LIST OF TABLES

LIST OF FIGURES

ABSTRACT

Wireless Underwater Communication Networks (WUCNs) have recently become a hot topic of research due to applications such as mine detection, navigation, and pollution monitoring. One-third of the earth's surface is covered by water, making it a challenging environment for communications. Acoustic waves are currently the most common technology used in underwater communications, but this approach suffers from large attenuation and propagation delays. Less commonly used are electromagnetic waves (EM), which experience range limitations in water, and optical waves, which encounter scattering. In this thesis, we will focus on magnetic induction-based communication. Magnetic induction (MI) has several advantages compared to the commonly used acoustic, EM, and optical communication methods. For instance, MI does not suffer from multi-path fading or scattering, and the signal propagation delay is negligible. We will roughly estimate the achievable range, operation frequencies, bandwidth, path loss, capacity and distortions of the MI in conductive media such as water.

LIST OF SYMBOLS USED

δ	Skin depth
ε	Electrical permittivity or dielectric constant
ε_0	Electrical permittivity of free space $\approx 8.85 \times 10^{-12}\ Fm^{-1}$
ε_r	Relative permittivity
λ	Wavelength
μ	Magnetic permeability
μ_0	Magnetic permeability of free space $\approx 4\pi \times 10^{-7}\ Hm^{-1}$
μ_r	Relative permeability
ρ	Mass density
σ	Electrical conductivity
ϕ	Specific aperture (merit factor)
ω	Angular frequency, $\omega = 2\pi f$
B	Flux density
c	Speed of light, $\approx 3 \times 10^8\ m/s$
f	Frequency
F_a	Atmospheric noise temperature
F_k	Atmospheric noise
H	Magnetic field
k	Boltzmann constant, $\approx 1.38 \times 10^{-23} Jk^{-1}$
k_0	Wave number for free space
m_d	Magnetic moment

N	Noise voltage or power
S	Signal voltage or power
T	Temperature [K]
T_a	Atmospheric noise temperature
Z_0	Wave impedance of free space, $Z_0 = \sqrt{\frac{\mu_0}{\varepsilon_0}}$

ACKNOWLEDGEMENTS

I would like to express my appreciation to my supervisor Schlegel who has cheerfully answered my queries, provided me with materials, checked my examples, assisted me in a myriad way with the writing and helpfully commented on earlier drafts of this project. Also, I am very grateful to my family and friends for their support throughout the production of this project.

CHAPTER1 INTRODUCTION

Traditional wireless networks that use EM suffer from high path loss, which limits their communication range. To increase the EM range, a large antenna is used for low frequencies, but this is unsuitable for small underwater vehicles. Optical waves experience multiple scattering, limiting the application of optical signals to short-range distances. Additionally, the transmission of optical signals requires a direct line of sight, which is another challenge for mobile underwater vehicles and robots [10]. Radio waves suffer from large attenuation and their range is limited to skin depth, which is associated with water conductivity. Seawater has high conductivity, but the salinity and physical properties of each type of seawater differ. Seawater measures around 4 S/m, whereas for pure water, typical values range between 0.005 and 0.01 S/m [4].

Acoustic waves are widely used in underwater communication because they can travel long distances. However, acoustic signals suffer from low bandwidth and data rates as well as large propagation delays because the sound speed equals 1500 m/s [10]. Magnetic induction (MI), however, is a promising solution for underwater short-range communication.

MI technology has already proved to be a useful tool for underwater exploration. Due to the high velocity of MI propagation, frequency offsets due to the Doppler effect are negligible. Time-varying magnetic induction, generated by a primary coil or loop and sensed by a secondary coil or loop, is the fundamental basis for magneto-inductive communications. Transformers consisting of two coils positioned very close to each other are the most common application of magnetic induction.

Ideally, total power is transferable from one coil to another. However, a regular magneto-inductive communication system featuring a large distance between primary and secondary coils rapidly experiences a power drop to a very small fraction. For this reason, coils are usually asymmetric, meaning that the transmitter coils are large and heavy, whereas the receiving coils are tiny and light [2]. A steering current drives the primary coil which generates a reactive magnetic field and makes MI communication possible. By using such a method, the energy stays local and is not transferrable at large distances that typical radio waves can propagate. Thus, because the receiving signal strength will experience a rapid decline over communication distance, it pushes MI communications out of the running as an alternative to regular wireless communications.

MI communication has the potential to be used for underwater communications, as less power loss occurs in comparison to electro-magnetic (EM) radio waves, which are rapidly absorbed in water. From a theoretical communication perspective, MI channels do not differ significantly from other electro-magnetic communication channels, and our approach is generally standard in communication theory. However, there are some differences between MI and RF communications, one of which is focusing on different physical characteristics of the environment when developing practical channel models for MI communications.

CHAPTER2 MI COMMUNICATION

MI communications use low-frequency modulation to enable reliable communication in areas where traditional radio-frequency (RF) communications fails. These environments include areas with a high concentration of conductive elements, through highly reflective barriers such as the surface of water and communicating through the earth. So far, MI communications has been limited to short ranges and low data rates but shows promise for providing high-data throughput at short ranges. The communication scenario provides unique opportunities and challenges. Additionally, given the nature of MI, it has not been fully explored, which means that current systems operate far below capacity.

2.1 Related Work

Magnetic induction was first introduced as an underwater tool in [6], which featured a high-speed link over a short range. In [8] and [1], underwater magneto-inductive networks were analyzed using mutual coupling. Developing a model for magneto-inductive communication was addressed in [7] by demonstrating the coupling between the coils in the near field. In [3], a narrow bandwidth of a few KHz was reported because of the high Q-factor (quality factor) of the magnetic coils. To expand the bandwidth [3], the front-end resonant frequency was modulated in [14]. In [10], tuned resonant circuits (narrowband) or unturned circuits (wideband) were applied to achieve high efficiency. Most of the literature, such as [13], [9] and [12], demonstrates channel modeling from an end-to-end perspective. So, for example, they focus not only the channel medium but also

on the characteristics of the transceiver and the coils. In this study, we focus on the channel as a medium.

2.2 Background

"Near field magnetic induction system is a short-range wireless physical layer that communicates by coupling a tight, low-power, non-propagating magnetic field between devices. The concept is for a transmitter coil in one device to modulate a magnetic field which is measured by means of a receiver coil in another device" [4]

In magneto inductive communications system, the distance of coils is usually larger, and transferred power drops off sharply to a very small fraction, so the coils should be asymmetric, which the transmitter coil being heavy and large, and the receiver coils being light and small. We are working in conductive media such as water, where the electrical conductivity σ leads to energy dissipation of the material because of the eddy current which generates strong secondary field. Electrical conductivity gives a measure of a material's ability to conduct an electric current.

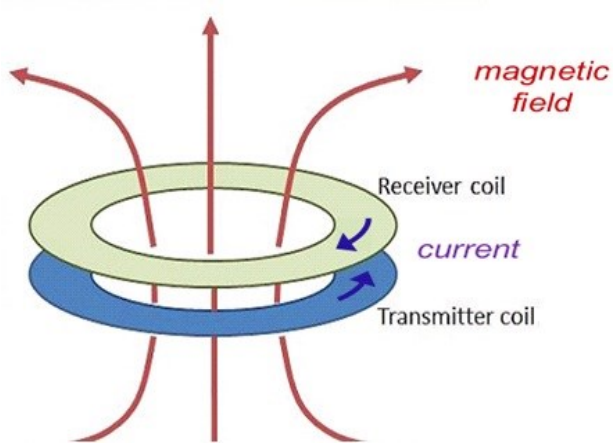

Figure 1 Inductive transmitter and receiver [4].

The principle of magnetic induction is the current in the primary coil (transmitter) generates magnetic field then the magnetic field induces current in to secondary coil (receiver). Magnetic flux is a general term associated with a field that is bound by a certain area. So, magnetic flux is any area that has a magnetic field passing through it. Electron has a magnetic dipole moment. It's close to an electric dipole moment because it generates a magnetic field that behaves similarly to an electric dipole field (falls off like 1 /r^3). The lowest order moment possible in magnetism that obeys Maxwell's equations is the dipole moment.

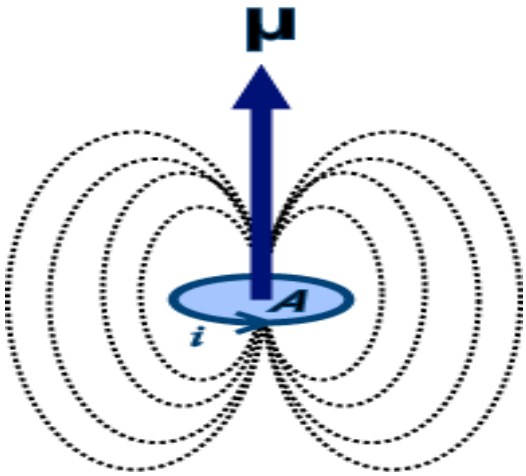

Figure 2 Magnetic moment [5].

According to Figure 2 When the current (*I*) traveling around the edge of a loop of cross sectional area (A=πr^2,where r is the loop radius), the magnetic moment will produce. The physics formula for calculating the dipole moment of a flat current carrying loop of wire is:

$$m_d = NIA \qquad (1)$$

where I is the current (Amperes) in the N turns, A is the area (m^2) of the loop, and N is the number of windings in the coil. The magnetic dipole moment (m_d) is a vector whose direction is perpendicular to A and determined by the right-hand rule. Thus, the unit of magnetic moment is (A m^2).

From (2), magnetic moment can be increased by increasing eitherN, I, A. However, by increasing N leads to more coupled core loss, as well as by increasing$I$, resulting more power losses (I^2R), also, increasing cross section area A, can lead to increase diameter and large antenna size is not practical for most applications. To increase magnetic field strength H, magnetic moment m_d could be enhanced by using magnetic permeability of the coil, given as,

$$m_d = \mu_e NIA \qquad (2)$$

Magnetic permeability μ determines the extent of magnetization obtained by the material in the presence of an external magnetic field and denoted by $\mu = \mu_0\mu_e$, where μ_0 is the permeability of free space, while μ_e is relative permeability of material, which various depending upon material type.

Clearly that magnetic moment depends on the number of turns, however the magnetic moment in relation to the mass and diameter, it is independent of the number of turns. For example, if we considering two magnetic loops A and B, loop A has 100 turns of wire, carrying a current of 4 A, with resistor 2Ω. we will compare loop A with loop B, where loop B has 500 turns and assuming both of loops have an identical mass.so loop B will

have five times the length of wire and resistance will be 25 times greater that is because five times greater due to length and another five times greater due to small cross section area. So, to get the same magnetic moment as loop A, it needs only 1/5 of the current (i.e. 0.8 A). Resulting in power dissipation I^2R for loop A is 32w as well as for loop B is 32w. The magnetic field strength $= \frac{m_d}{4\pi r^3}$, at a coaxial point at distance r from the loop antenna is proportional to the magnetic moment and decreases with the third power of r. Magnetic field strength can be increased by increasing magnetic moment.

CHAPTER3 METHODOLOGIES

The methodologies we are adapting here quite standard in the field of communication theory.

3.1 The Magneto Inductive Channel

The MI channel fundamentally includes the MI transmitter, the magnetic channel in conductive media, and the MI receiver. These are shown in the block diagram in Figure 3 and discussed individually below.

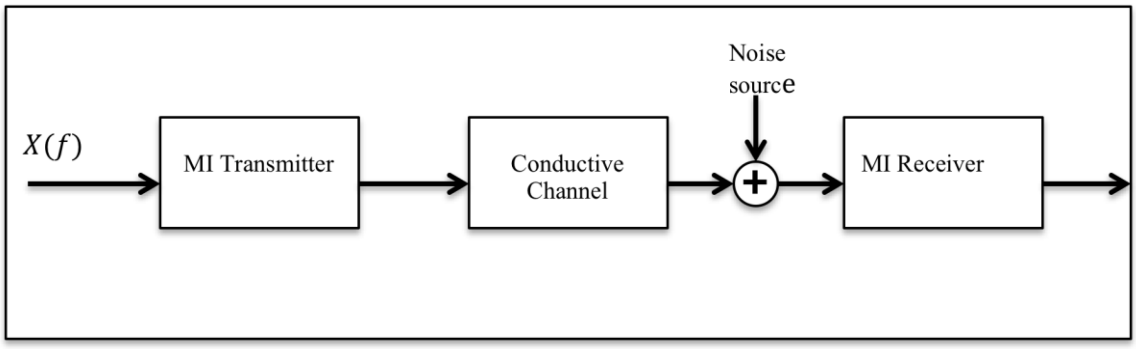

Figure 3 Model of a magneto-inductive communication system.

3.1.1 The Magneto Inductive Transmitter

An inductive loop is the most practical and efficient way to generate a magnetic field [2]. The magnetic field from the loop antenna falls into the following three regions: the near field region, in which the field is described by quasi-static equations and there is no significant radiation as the electric and magnetic fields are in phase quadrature; the far field, which represents the region where the electric and magnetic fields are in phase and where

the magnetic field peels off as a propagating electro-magnetic wave; and the transition region, which is located between the near and far field regions [2].

Table 1 Showing the boundary conditions of the near field, transition zone, and far-field.

Properties	**Near–field approximation**	**Transition region approximation**	**Far-field approximation**
Skin depth	$T \ll 1$	$T^2 \ll 1$	$T \gg 1$
Wave number	$k_0 r \ll 1$	$(k_0 r)^2 \ll 1$	$k_0 r \gg 1$

As we can see from Table 1 boundary conditions of the three regions using two common measures (wavenumber $|\boldsymbol{k_0}|$and skin depth $\boldsymbol{\delta}$), where is the $\boldsymbol{T}$ the ratio of distance to skin depth, given as $\boldsymbol{T} = \frac{\mathbf{r}}{\boldsymbol{\delta}}$ and $\boldsymbol{k_0} = \frac{\mathbf{2\pi f}}{\mathbf{c}}$. We are primarily interested in the near field, for which $\mathbf{r} < \boldsymbol{\delta}$ and

$$\mathrm{T} = \frac{\mathrm{r}}{\delta} < 1 \qquad (3.1)$$

where r is the operating distance and T is skin depth numbers.

The magnetic near-field decays with the inverse cube of the distance. According to the Biot – Savart Law, the magnetic field from a small element is proportional to $(\frac{1}{r^3})$.

$$\boldsymbol{B} = \frac{\boldsymbol{\mu_0}}{\boldsymbol{4\pi}} \int \boldsymbol{I} \frac{\boldsymbol{dI \times r}}{\boldsymbol{r^3}} \qquad (3.2)$$

where B is the flux density and I is the current (see Figure 4).

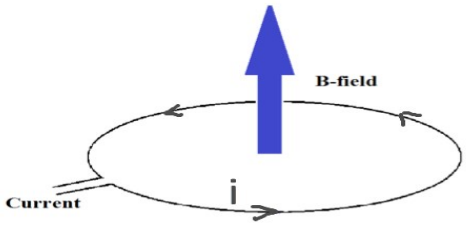

Figure 4 Illustration of a loop antenna at the transmitter side.

The magnetic field strength for induction at a distance r from the loop antenna is proportional to the magnetic moment and decreases with the third power of r, given by

$$H = \frac{m_d}{4\pi r^3} \tag{3.3}$$

where m_d is the magnetic moment for a circular loop antenna given by

$$\boldsymbol{m_d = \frac{d_t}{4}\sqrt{M\frac{\sigma}{\rho}}\sqrt{p} = \phi_t\sqrt{p}} \tag{3.4}$$

p is the dissipated power, and ϕ_t is the antenna merit factor, given by

$$\boldsymbol{\phi_t = \frac{d_t}{4}\sqrt{M\frac{\sigma}{\rho}}} \quad . \tag{3.5}$$

In the above, ϕ_t depends on the mass $M$of the coil, the diameterd_t, the electrical properties of the wire material, which are the conductivity σ, and the material density ρ. These parameters are collected in the antenna merit factor ϕ_t, which has dimensions $m^2/\sqrt{\Omega}$. The magnetic moment also depends on the dissipated power p, but does not depend on the number of turns [3].

For example, consider a portable induction loop antenna, where the diameter is 1m and mass is 0.6 Kg. If we take into account that the loop is made from copper $\sqrt{\frac{\sigma}{\rho}}$=8m/Kg$\sqrt{\Omega}$, the magnetic moment is 50 Am^2 with a power dissipation of 10 w.

The H-field is directly proportional to the loop current. Hence, since the power loss in the antenna (which is due to ohmic resistance) is also directly proportional to the loop current, there is no fundamental preference of frequency [2].

3.1.2 The Communications Channel

Communication through conductive media such as seawater is possible only over distances of a few skin depths. The skin depth gives a measure of the penetration of magnetic field into a given medium. The magnetic field decays with distance into the medium, and this decay of the field is expressed by the skin depth, given by [3]

$$\boldsymbol{\delta} = \sqrt{\frac{\mathbf{2}}{\boldsymbol{\omega\mu\sigma}}} \qquad (3.6)$$

where:

$\mu = 4\pi \times 10^{-7} \quad N/A^{-2}$ (Magnetic permeability in vacuum)

$\omega = 2\pi f$ (Angular frequency)

σ : Electrical conductivity in siemens/meter

The penetration of the magnetic field into the conductive medium obeys Maxwell's equations:

$$\triangle \times \boldsymbol{H} = (\boldsymbol{j\omega\varepsilon} + \boldsymbol{\sigma}). \qquad \text{(Ampere's law)} \qquad (3.7)$$

Electromagnetic waves in a vacuum obey a standard type of partial differential equation (PDE) called the "wave equation". However, in a conductive medium, where the angular frequency is much less than sigma/epsilon, they obey a different type of partial differential equation, known as the "diffusion equation".

If $\omega \ll \sigma/\epsilon$, the propagation equation of the magnetic field turns into the diffusion equation, which means diffusion properties of electromagnetic waves are mainly dependent on the conductivity and propagation behavior of the wave is an important aspect of time.

$$\triangle^2 \boldsymbol{H} = \boldsymbol{j\omega\mu\sigma H}. \tag{3.8}$$

The magnetic field is attenuated according to the skin depth. In a good conductor with $(\frac{\sigma}{\omega\varepsilon} \gg 1)$, such as seawater, a large skin depth attenuation is experienced. If we assume an operating frequency of 1 MHz, the skin depth for seawater is 0.25m with a wavelength of 1.6m. This means the frequency within the LF (30-300 kHz) or the VLF (3-30 kHz) bands would be the most optimal, as skin depth is inversely proportional to the square root of the frequency used.

A basic model for the magnetic field penetration consists of a cubic distance attenuation combined with an exponential absorption loss given by [2]

$$|\boldsymbol{A}(\boldsymbol{\omega}, \boldsymbol{r})| = \frac{\mathbf{Q(T)}}{\mathbf{4\pi r^3}} \ . \tag{3.9}$$

The attenuation Q(T) represents the exponential medium losses at a rate of 8.7 dB per skin depth. It is frequency-dependent, since δ is frequency-dependent and has general low-pass characteristics. It is given by

$$Q(T) = 2e^{-T}\sqrt{T^2 + (1+T)^2}. \tag{3.10}$$

The total absorption is the combination the cubic distance attenuation of (3.9) and the exponential absorption loss in (3.10).

3.1.3 The Magneto -Inductive Receiver

A receiver for magneto -inductive communications basically consists of a secondary loop antenna that is coupled with the first loop antenna [3].

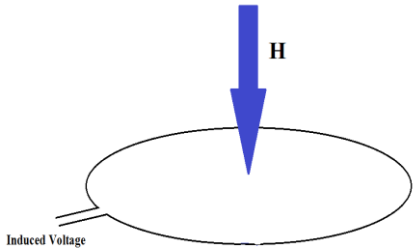

Figure 5 Illustration of the second loop at the receiver.

The induced voltage in a receiver coil via Faraday's law due to the AC magnetic flux density produced by a magnetic dipole source as a function of frequency, distance and material parameters, is given by

$$\boldsymbol{U(f) = 2\pi f \mu H \phi_r} \qquad (3.11)$$

where H is the magnetic field component at the receive loop and $\phi_r$is the receiver antenna loop merit factor. The induced voltage also depends on magnetic permeability $\mu = \mu_{eff}\mu_0$, where μ_0 is the magnetic permeability of free space $\approx 4\pi \times 10^{-7}$ Hm^{-1}, and $\mu_r = 1$ because most of the materials are not ferromagnetic.

In a good conductor with ($\frac{\sigma}{\omega\varepsilon} \gg 1$), and if the communication range is within the near field, ($T \ll 1$), the optimal frequency for a given distance r is given by

$$f = \frac{T^2}{\pi r^2 \mu \sigma} \quad . \tag{3.10}$$

by substituting (3.12) in (3.11) to derive the induced voltage in a coaxial receiver loop as

$$U_{induced} \approx \phi\sqrt{R}\frac{m_d}{2\pi\sigma} . \frac{1}{r^5} \quad T^2 \quad Q(T) \quad . \tag{3.11}$$

As the frequency goes to zero, the skin depth δ becomes large and T→ 0 so the induced voltage tends to zero. This is due to the lack of magnetic induction at frequency 0. Likewise, at a high frequency, δ becomes small and T → ∞ so $e^{-T} \rightarrow 0$. As a result, there is no signal because of the greater degree in skin depth attenuation [3].

3.2 Channel with Noise

The term 'noise' refers to unwanted electrical signals that are always present in electrical systems. Signal transmission through any channel suffers from additive noise, which can be generated internally by the components such as resistors and solid-state devices used to implement the communication system. This is called thermal noise. Such noise can also be generated externally as a result of interference from other channel users. Noise is one of the limiting factors in a communication system because when noise is added to the signal, it is impossible to transmit a near infinite amount of information over a finite bandwidth communication system.

3.2.1 Thermal Noise

Thermal noise is generated due to the random movement of electrons inside the volume of conductors or resistors even in the absence of electric field. If the noise at the receiver is purely thermal, its normalized noise power spectral density is given by:

$$N(f) = 4kT \tag{3.14}$$

where $k = 1.38 \times 10^{-23}$ J/K is Boltzmann's constant, and T is the receiver temperature in Kelvin [2].

3.2.2 Atmospheric Noise

Atmospheric noise is a collective term of all noise sources that are not local thermal. A typical example of atmospheric noise is receiver noise. It may be caused by the electrical activity in the atmosphere as well as by man-made electrical disturbances. In lower frequency ranges, ambient noise is picked up by the antenna, especially if the antenna is at the surface and dominates over thermal noise. Therefore, it is preferable to use a noise model that is analogous to the thermal noise. In the following, we define the atmospheric noise power density as

$$N(f) = 4kTF_a(f)\, R_r/R \tag{3.15}$$

where R_r is the radiation resistance of the antenna, R is the ohmic resistance of the receiver coil, and F_a is the atmospheric noise temperature given by

$$F_a(f) = \frac{6\pi}{k_0^2}\frac{Z_0 H^2}{4kT} \quad (3.16)$$

where k_0 is the wave number and is equal to $k_0 = \frac{2\pi f}{c}$ (where c is the speed of light) and Z_0 is the impedance of free space. Z_0 also equals the ratio of the electric field component to the magnetic field component $Z_0 = \frac{|E|}{|H|}$ and is approximately 377 Ohm.

We can use (3.16) to deliver the atmospheric noise as a function of frequency and atmospheric noise temperature in the following

$$F_k = \sqrt{F_a \frac{Z_0 k_0^4}{6\pi}} \quad (3.17)$$

$$20logF_k = 10logF_a + 40logf - 294.147 \quad (3.18)$$

3.3 Channel Capacity

Long before wireless communication dominated our daily lives, research had established fundamental limits on the rate at which we could communicate over wireless channels. One of the most important theorems is the Shannon capacity theorem, which sets an upper bound on how fast we can transmit information over a particular wireless link. There is no way to exceed this theoretical upper bound, but we can get close to it.

The Shannon capacity formula for a flat channel with white Gaussian noise is given by

$$\boldsymbol{c = wlog_2(1 + \frac{s}{N})} \quad (3.19)$$

where w is Bandwidth in (Hz) , and $\frac{S}{N}$ is the signal –to- noise ratio.

The capacity is directly proportional to the bandwidth. If we have a wider bandwidth to communicate, we can send more data. This is important because we will look at how bandwidth is allocated in terms of different frequency bands.

We can generalize instances of frequency-dependent signals and noise spectral powers $S(f)$ and $N(f)$ in the following way:

$$c = \sum_{i=0}^{N} \Delta f \log(1 + \frac{S(f_1+i\Delta f)\Delta f}{N(f_1+i\Delta f)\Delta f}) \rightarrow \int_{f_1}^{f_2} \log(1 + \frac{S(f)}{N(f)})\, df \qquad (3.20)$$

where f_1 is the lower band edge, $f_2=f_1+N\delta f$ is the upper band edge, and $f_2-f_1=w$ is the channel bandwidth.

CHAPTER4 RESULTS AND DISCUSSION

In this study, all the graphs are done by using Matlab software and some of our results are summarized into tables.

4.1 MI Channel

Frequency should be as low as possible to avoid eddy current which produce strong secondary field. skin depth is frequency dependent (3.6), so in Figure 6 will show the skin depth as a function of frequency for seawater ($\sigma = 4S/m$) and fresh water ($\sigma = 0.01S/m$).

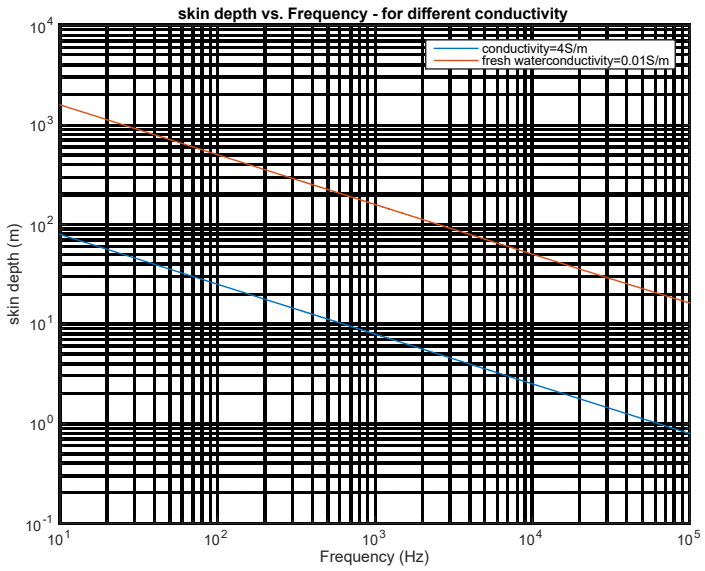

Figure 6 Skin depths as a function of frequency and conductivity for both seawater and fresh water.

According to Faraday's law, the induced signal will be smaller at low frequencies; however, there will be less signal attenuation at those frequencies due to skin effect [3]. Figure 7 shows the induced voltage at the inductive loop given by (3.11), where is ϕ_r =1 $m^2/\sqrt{\Omega}$ and $m_d = 75$ Am^2, and plotted up to ($k_0 r \ll 1$), the amplitude of the voltage induced in a coil increases with frequency, as dictated by Faraday's law of induction

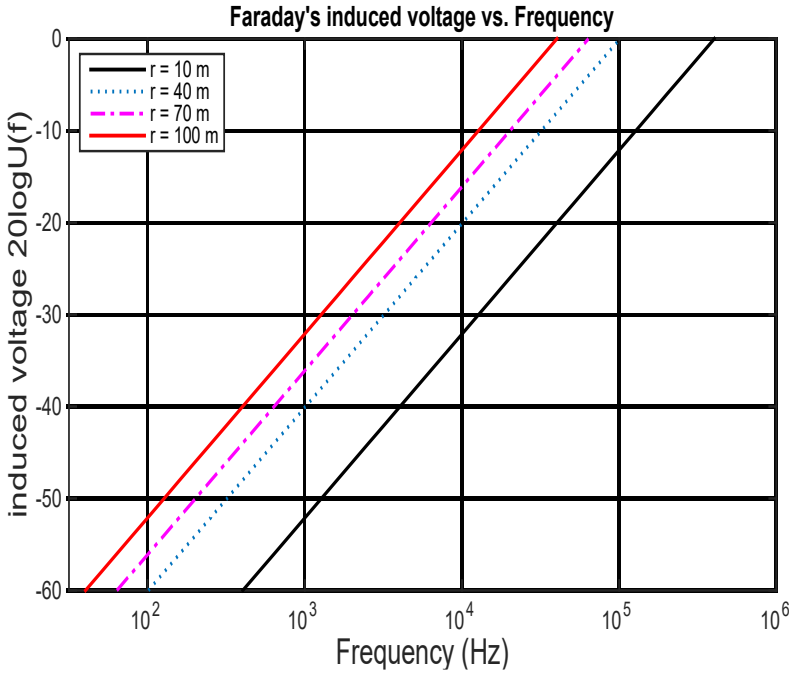

Figure 7 Induced received voltage as a function of frequency for different separation distances between T_x and R_x.

Figure 8 will show the case of the induced voltage combined with the field decay and the exponential decay term e^{-T} for different penetration depths, where is $\phi_r = 1$ m^2 $/\sqrt{\Omega}, m_d = 75$ Am^2 and σ=4 S/m and plotted up to($k_0 r \ll 1$).

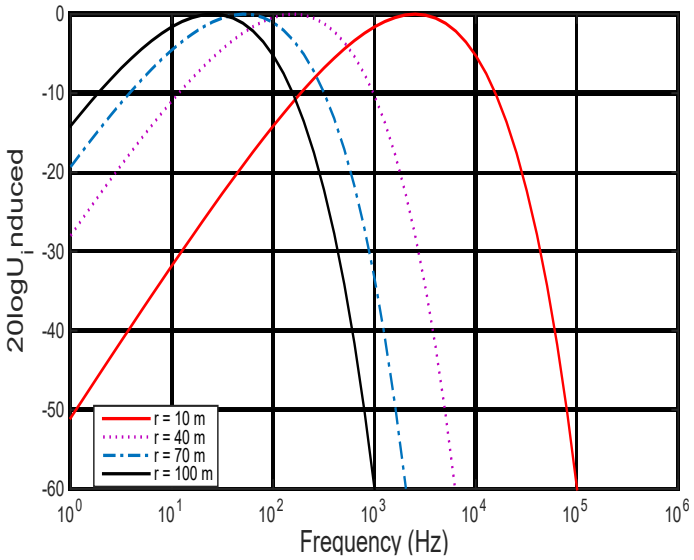

Figure 8 Induced voltages for a coaxial receiver loop as a function of frequency for different separation distances between T_x and R_x.

Sea water is considered a good conductor, where $\frac{\sigma}{\omega\varepsilon} \gg 1$[11], this indicates that for frequencies well within the near field ($k_0 r \ll 1$), a band-pass behavior is seen (Figure 8) because of the interplay between Faraday's law of induction in (3.13) and the exponential attenuation in (3.10).

4.2 Channel Attenuation

In MI, the channel attenuation is calculated by combining the cubic distance and the exponential absorption, given in (3.9).

Figure 9 shows the attenuation $|A(\omega, r)|$ of an MI channel as a function of distance and frequency for seawater with a typical value of $\sigma = 4S/m$.

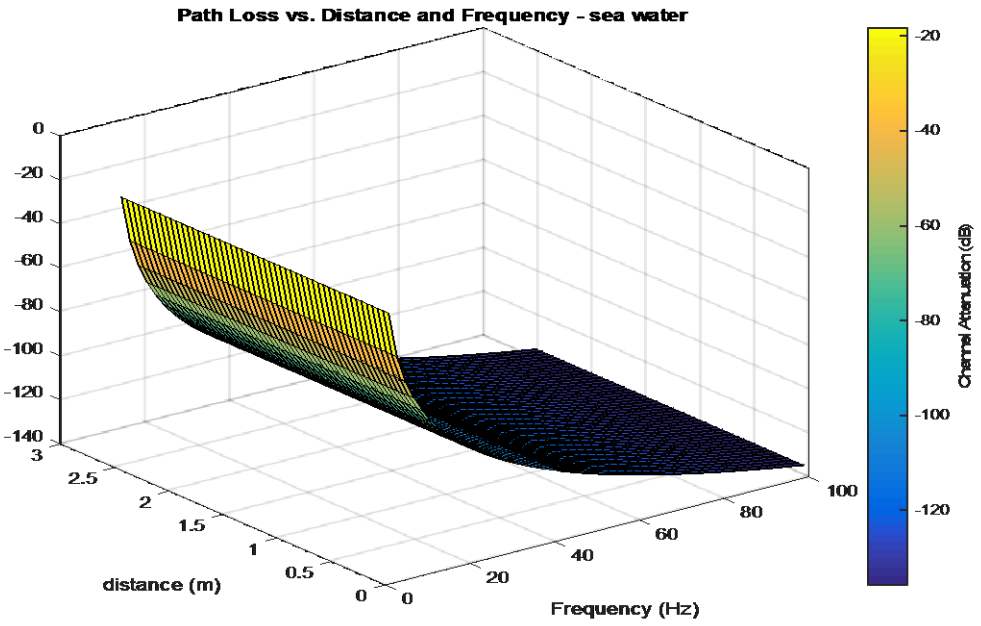

Figure 9 Distance and frequency dependent attenuation of the magneto-inductive signal for a typical value of σ=4S/m for seawater.

We modified the previous simulation (which is not valid for making the decision) from 3-dimensional to 2-dimensional (see Figure 10). Our reason for doing this is that the skin depth depends on the frequency while the T ratio depends on distance and skin depth, and different frequencies can cover different distances. Furthermore, when we plot all frequencies together, higher frequencies need a lower skin depth and a lower distance, whereas lower frequencies need higher skin depth and longer distance. Therefore,

integrating both high and low frequencies in the same plot and ensuring that all are "near-field" regions means that we should stick to the simulation of the lowest distance, which can be accessed by the highest frequencies. Thus, we changed the code and performed the simulation for different frequencies over a distance that can meet near-field criteria.

The simulations in Table 2 were done using the MATLAB script "SkinDepth - Equ_88_v2.m" and all results are stored in the "MI figures" folder. Table 2 reflects the essence of these results, showing the maximum distance reachable in seawater and fresh water for different frequencies. It is worth noting that the T ratio is set at $r < 0.2\delta$ in order to ensure that the simulations and results are in the near field. There is a possibility to obtain better distance if we compromise the ratio T with higher values.

Table 2 The results of reaching maximum distance for different frequencies in both fresh and sea water, and in the near-filed region (**T**=0.2).

	f = 1 (Hz)	**f = 10 (Hz)**	**f = 100 (Hz)**	**f = 1,000 (Hz)**	**f = 10,000 (Hz)**	**f = 100,000 (Hz)**	**f = 120,000 (Hz)**	**f = 140,000 (Hz)**
Max depth penetration in Seawater (m)	50	16	5	1.6	0.5	0.16	0.14	0.13
Max depth penetration in Fresh water (m)	1000	320	100	32	10	3.3	2.9	2.7

The maximum frequency for staying in the near-filed in fresh water is around 145 kHz, since increasing the frequency might push T out of near field. However, the maximum frequency for staying in near-field for sea water could be more than 1 MHz or higher, as sea water does not have the limitation of fresh water; however, the range will be reduced and cannot be considered as an option for communication.

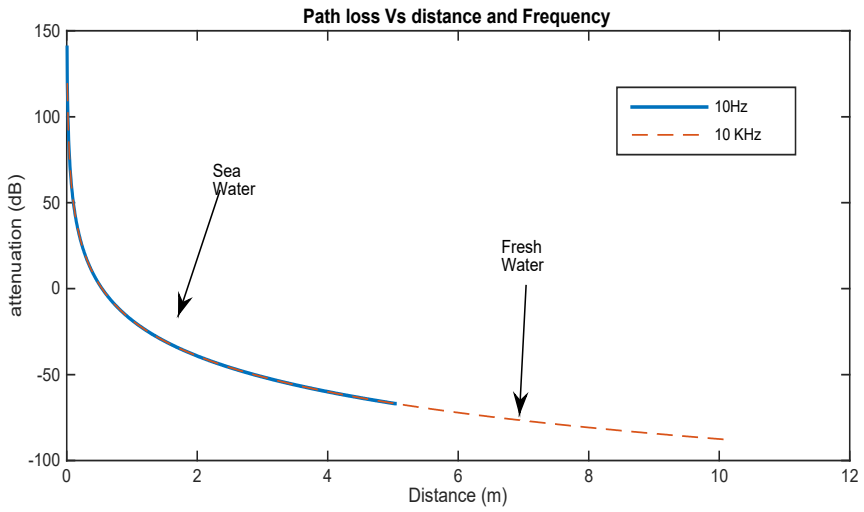

Figure 10 Illustration the channel attenuation in seawater with $\boldsymbol{\sigma = 4s/m}$ and in fresh water with $\boldsymbol{\sigma = 0.01s/m}$.

The proper range for communication under water could be achieved at lower frequencies, but the attenuation is too great and an acutely sensitive receiver might be needed. If we set the maximum attenuation to -60 dB, the best option for communication will be frequencies up to 10 kHz, The achievable communication range is around 10 meters for fresh water and around 10 Hz with achievable distances of around 5 meters in sea water (These results are observable from the MI figures named s1, f1, s10, f10, s1000, f1000, etc. located in MI figures folder).

By studying the simulations in this phase, we can verify the fact that the channel has a strong low-pass characteristic, especially at larger distances.

In terms of channel attenuation, simulations in Figure 11 show the result for both sea and fresh water. The antenna merit factor product equals 100, inclusive, in that $\phi_t = 100$ m^2 /$\sqrt{\Omega}$ and $\phi_r = 1$ m^2 /$\sqrt{\Omega}$, with reference transmit power of 1 W.

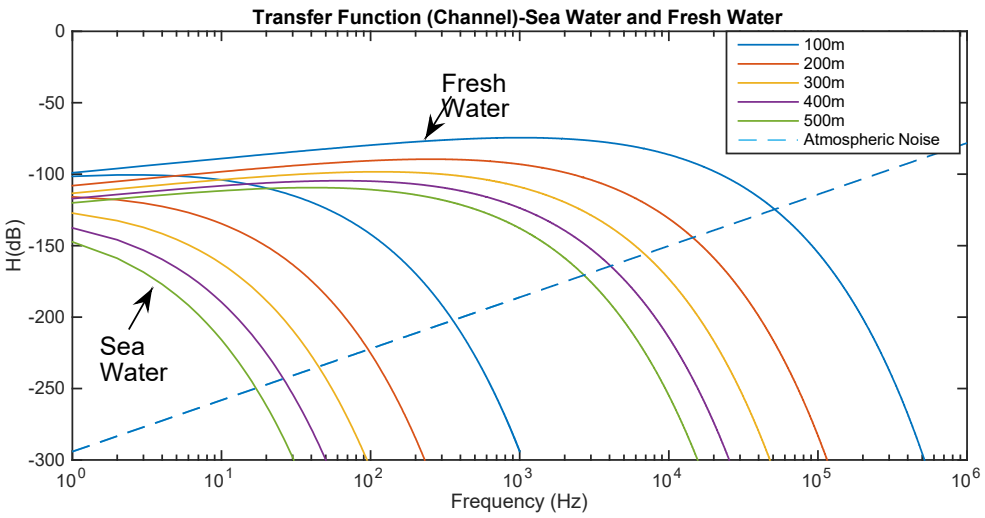

Figure 11 System transfer function $\boldsymbol{H(f)}$ with different penetration depths for both seawater and fresh water.

In Figure 11, for both seawater and fresh water, atmospheric noise refers to atmospheric noise temperature. The reference power is also 1 w (0 dBW). It should be noted that the optimal transmission range depends on the received SNR, which itself depends on the transfer function as a distance dependent factor (more distance, more attenuation) and the transmitter power. We can see this by looking at Figure 11 and setting the first necessity as a channel with a flat bandwidth. Tables 4 and 5 reflect the details of the channel bandwidth over different ranges of communications for sea and fresh water, respectively. The bandwidth has been calculated using Figure 11. The -3dB bandwidth occurs when the channel attenuation drops for 3dB from its value at f=1KHz. So, for example, for seawater with a communication range of 100m, the attenuation at f=1Hz is -101.5 dB. Thus, the -3dB bandwidth occurs when the attenuation drops an extra 3dB(-101.5 –3 = -104.5 dB). The point (around 10 Hz) can be found in Figure 10. By performing the same calculations for all frequencies in both seawater and fresh water, the results would be as shown in Tables

4 and 5. The channel attenuation is considered the channel attenuation at -3dB point, which is 3dB less than the attenuation at f=1 Hz.

Table 3 Channel Characteristic-Seawater.

Communication Range (m)	**Bandwidth (Hz)**	**Channel Attenuation (dBW)**
100	10	-101.5-3=-104.5
200	2	-115.9-3=-118.9
300	<1	-127.3-3=-130.3
400	<1	-137.6-3=-140.6
500	<1	-147.3-3=-150.3

Table 4 Channel Characteristic-Fresh water.

Communication Range (m)	**Bandwidth (Hz)**	**Channel Attenuation (dBW)**
100	100000	-99.01-3=-102.1
200	10000	-108.1-3=-111.1
300	2000	-113.4-3=-116.4
400	900	-117.1-3=-120.1
500	800	-120.1-3=-123.1

As we can see by comparing Tables 3 and 4, a very good bandwidth could be achieved in fresh water communication.

4.3 Channel Noise

The signal-to-noise ratio (SNR) is an important coefficient to determine a system's performance. The SNR at the receiver loop given by

$$\left.\frac{S}{N}\right|_{\substack{thermal+\\ atmosheric}} = \frac{\omega\mu H}{\sqrt{4kTB}}\phi/\sqrt{1+(\phi F_k)^2} \quad . \tag{4.1}$$

In (4.1), we can clearly see that there are two conditions to calculate the SNR. First, if the antenna is too small (which means the merit factor ϕ is extremely small), the thermal noise dominates over the atmospheric noise and the atmospheric part of the noise can be ignored. Second, if the antenna is very large, the specific aperture will be large. Atmospheric noise must be taken into account because it has a strong effect on system performance.

1) When $F_k\phi < \frac{1}{2}$, the SNR will approximately be given by

$$\left.\frac{S}{N}\right|_{\substack{thermal+\\ atmosheric}} \approx \frac{\omega\mu H}{\sqrt{4kTB}}\phi \ . \tag{4.2}$$

2) When $F_k\phi > 2$, the SNR is given by

$$\left.\frac{S}{N}\right|_{\substack{thermal+\\ atmosheric}} \approx \frac{\omega\mu H}{\sqrt{4kTB}}/F_k \quad . \tag{4.3}$$

From (4.3), we note that the SNR is independent of the merit factor ϕ.

Figure 12 demonstrates the SNR (4.1) by considering both thermal and atmospheric noise for various communication ranges and different distances. The assumption of the antenna merit factor is 50 $m^2/\sqrt{\Omega}$ and the reference transmit power is 1 W.

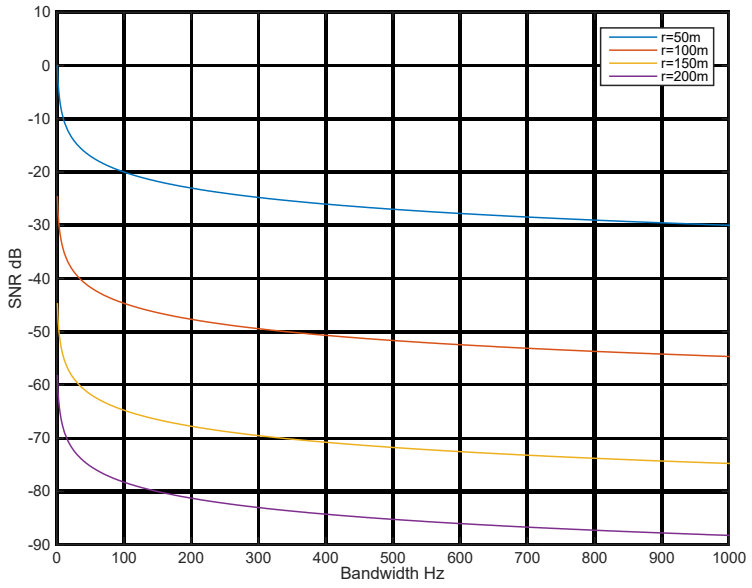

Figure 12 SNR for various communication ranges and different penetration depths.

Figure 13 shows the SNR for various communication ranges. Both (4.2) and (4.3) use a merit factor of 50 $m^2/\sqrt{\Omega}$, and reference transmitter power of 100 W. With the factor $\sqrt{\frac{\rho}{\sigma}} = 117$.

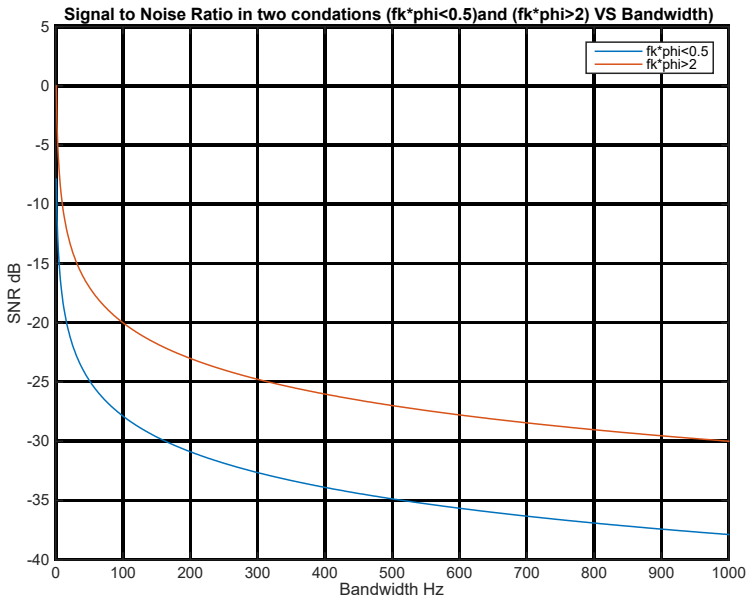

Figure 13 SNR for seawater with $\boldsymbol{\sigma = 4s/m}$, figure shows two conditions when $\boldsymbol{F_k\phi < 0.5}$, and $\boldsymbol{F_k\phi > 2}$.

The merit factor plays an important role in the system performance. For example, consider a small induction loop with a merit factor 10 $m^2/\sqrt{\Omega}$. If we apply an operating frequency of 85 KHz and power of 50 W, the radiated power P_r will be quite small and equal to 1 μW. However, for the same operating frequency and power with a merit factor of 100 $m^2/\sqrt{\Omega}$, the radiated power will be 1.12 mW, as in the following

$$P_r = m_d^2 \frac{z_{0k_0^4}}{6\pi} \quad . \tag{4.4}$$

Atmospheric noise in lower frequency ranges could be picked up by the antenna. Hence, if the merit factor is greater than 0.25, the thermal noise can be ignored and only atmospheric noise should be taken into account [2], [3]. A simple approximation of the atmospheric noise temperature can then be used as in the following:

$$N(f) = 4kTF_a(f)\phi^2 \frac{k_0^4 z_0}{6\pi} \quad (4.5)$$

where $Z_0 = \sqrt{\frac{\mu}{\epsilon}} \approx 377\Omega$, and $k_0 = \frac{2\pi f}{c}$ by substituting the constants into (4.5). Thus, the modified equation will be:

$$N(f)dB = 10log_{10}(6.1633 \times 10^{-50} \times f^4) + 10log_{10}(\phi^2) + F_a(f)(dB) \quad (4.6)$$

We can calculate the SNR by using (Power_r_x = Power_t_x + Channel attenuation) and Power_noise = Power_atmospheric_noise. This degrades the "Power_r_x" by 30 dBW, where Power_t_x = 1 w, which is 0 dB (see Tables 5 and 6).

By finding the SNR, we can calculate the capacity from the Shannon capacity formula for a flat channel with white Gaussian noise (3.6).

Table 5 Capacity calculations for Seawater MI communication.

Communication Range (m)	**S (dB) P_t_x + Channel Attenuation**	**N (dB) Atmospheric noise**	**SNR**	**Bandwidth W**	**C (bps)**
100	0 -104.5	~ -154	49.5	10	~ 164
200	0 -118.9	~ -157	38.1	2	~ 25
300	0 -130.3	< -158	< 27.7	<1	< 9
400	0 -140.6	< -158	< 17.4	<1	< 5
500	0 -150.3	< -158	< 7.70	<1	< 2

Table 6 Capacity calculation for Fresh water MI communication.

Communication Range (m)	***S (dB)*** P_t_x + ***Channel Attenuation***	**N (dB) Atmospheric noise**	**SNR**	**Bandwidth W**	C **(bps)**
100	0-102.1	~ -140	37.99	100000	315,510
200	0-111.1	~ - 143	31.90	10000	48,326
300	0-116.4	~ -145	28.6	2000	15,946
400	0-120.1	~ -146	25.9	900	6938
500	0-123.1	~ -147	23.9	800	3639

Note that the Capacity and communication range are significantly better for fresh water communication.

4.4 Up-link and Downlink Operation

The main impact of atmospheric noise is on uplink and downlink operations, with the effect being different for the uplink compared to the downlink. Specifically, in the uplink, the full value of atmospheric noise will be present, while in the downlink, atmospheric noise will attenuate as 8.7 per skin depth.

In this example (Figure 14), we will consider communication between a boat located on the surface and diver carrying the other coil. The maximum depth for divers to communication will be 50m.

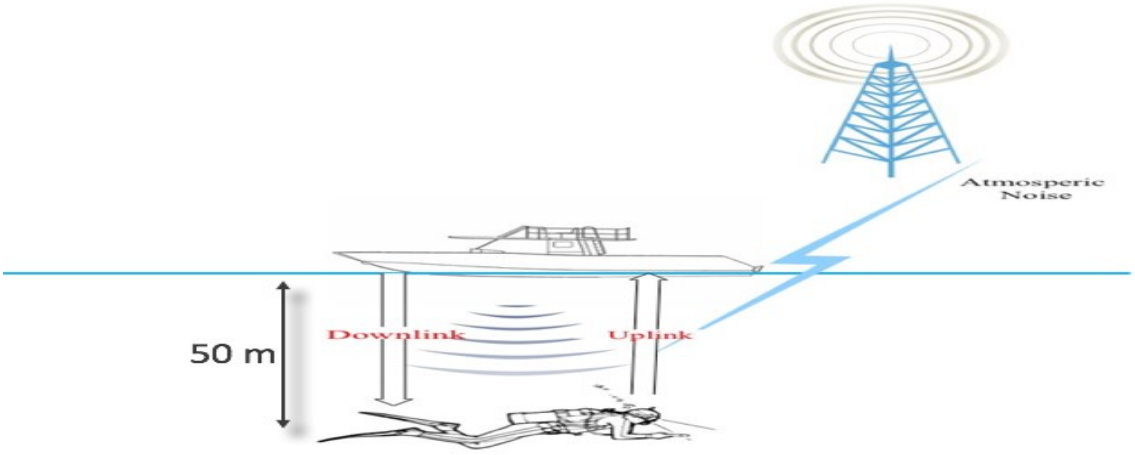

Figure 14 Example 1 on uplink and downlink communications.

The merit factor based on [2][3] should be greater than 0.25, so we can ignore the thermal part of the noise and $F_a(f)(dB) = 294.15 - 36\log(f)$. Hence, to obtain a merit factor of at least 0.25, we can choose antennas as below

Boat antenna specifications: r=2m, M= 4 Kg, $\sqrt{\sigma/\rho}$ = 50, which can give us $\emptyset_b = 100$

Diver antenna specifications: r=0.1m, M= 1 Kg, $\sqrt{\sigma/\rho}$ = 20, which can give us $\emptyset_d = 1$

So, in this case, $\emptyset = \emptyset_b \times \emptyset_d$ = 100, which is greater than 0.25, and all assumptions and approximations are valid. Because the merit factor is collected the diameter, mass and material parameters so if merit factor is small that means loop antenna is small and in this case, we can ignore atmospheric noise taking in our account just thermal noise, however, if merit factor is big meaning that antenna size is big and we can ignore thermal noise because to its insignificant against atmospheric noise.

The communication range is maximum 50m, and since we are working in near-field and T<<1 (T=0.2 in our MATLAB code), $T = \frac{r}{\delta} << 1$, as we assumed 0.2 during our previous simulations.

Next, in finding $\delta = \frac{50}{0.2} = 250$ m, we need to find the maximum working frequency $\delta = \sqrt{\frac{2}{\omega\mu\sigma}}$. By making frequency the main subject, we will have $= \frac{1}{\pi\delta^2\mu\sigma}$; if we solve it, we will get maximum frequencies for fresh and seawater, as below:

The minimum working frequency for seawater = 2 Hz, while the minimum working frequency for fresh water = 406 Hz.

Basically, for data communication or even voice communication, the actual situation is when the channel offers a flat attenuation over the transmitted signal bandwidth; however, in reality, achieving a flat attenuation is not possible, as attenuation is frequency-dependent. Therefore, we will first offer a solution for strict flat attenuation, and then we will modify it to the real situation when the channel can be considered, even when it experiences a steep roll off. In the latter case, the transmitter power and the SNR can gauge the communication range and bandwidth. On the receiver side, some type of channel equalization will definitely be needed; however, this is outside the scope of the present topic.

To sum up, the first scenario needs a simple receiver, but it has a limited transmission bandwidth, whereas the latter scenario can offer a better communication bandwidth at expense of receiver complexity.

The uplink system presents the full value of atmospheric noise to the receiver. The diver coil transmission power is 0 dB for initialization, giving the following calculations:

Channel loss (which consists of a cubic distance attenuation combined with an exponential absorption loss due to skin depth) calculation by using MATLAB (SkinDepth _Equ_88_V4.m). The results are shown in tables below.

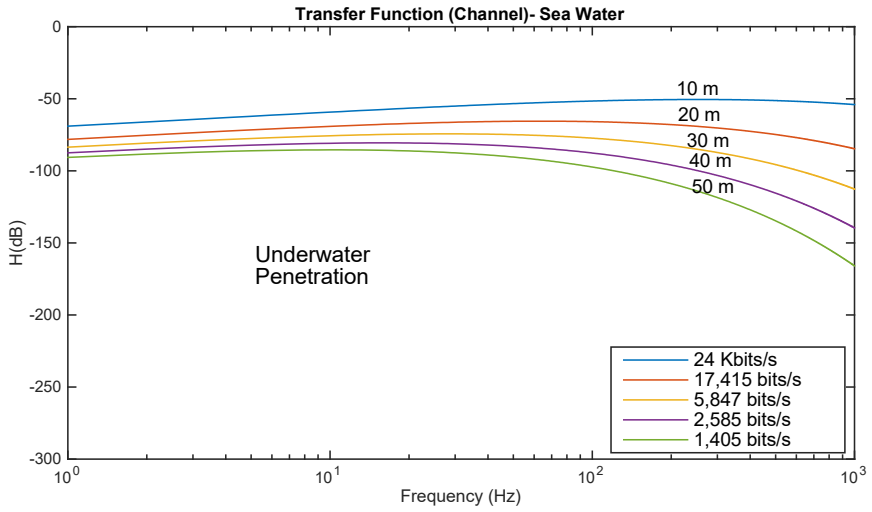

Figure 15 Flat attenuation uplink (SNR)-Seawater (Example1).

Table 7 Channel characteristics (flat attenuation)-Seawater.

Communication Range (m)	**Bandwidth (Hz)**	**Channel Attenuation (dB)**
10	> 1000	< -69.02 -3=-72.02
20	810	-78.12-3=-81.12
30	284	-83.53-3=-86.53
40	132	-87.48-3=-90.48
50	73	-90.64 – 3 = -93.64

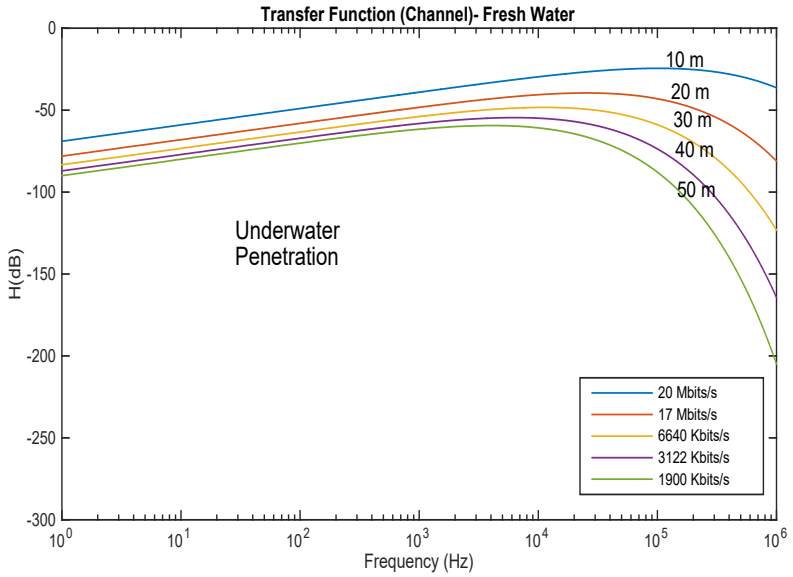

Figure 16 Flat attenuation uplink (SNR)-Fresh water (Example1).

Table 8 Channel characteristics (flat attenuation)-Fresh water.

Communication Range (m)	**Bandwidth (Hz)**	**Channel Attenuation (dB)**
10	> 1000000	<-69.01-3=-72.01
20	~ 1000000	-78.04-3=-81.04
30	~ 400000	-83.32-3=-86.32
40	~ 200000	-87.07-3=-90.07
50	~ 125000	-89.98-3=-92.98

Because the results shown in Tables 7 and 8 might appear somewhat confusing, further explanation will be provided here. For instance, the SNR for a 50m communication range in seawater is higher than that for fresh water (93.64 dB compared to 92.98 dB). However, the strict and flat bandwidth achievable for seawater in the range of 50m is less than 100

Hz, while this bandwidth exceeds 125 KHz in the case of fresh water. Thus, the quality of communication differs significantly here.

For the downlink system case, the atmospheric noise experience attenuation as it propagates down through the medium of either fresh water or seawater. The attenuation model is the same as the signal attenuation model. Here again, the boat coil transmission power is 0 dB for initialization. Channel loss (which consists a cubic distance attenuation combined with an exponential absorption loss due to skin depth) is calculated by using MATLAB (SkinDepth_Equ_88_V4.m) and the results are shown in Tables 9 and 10

Table 9 Flat attenuation downlink (SNR)-Seawater (Example1).

Communication Range (m)	**S (dB) = P_tx + Channel Attenuation**	**N (dB) Attenuated Atmospheric Noise**	**SNR (dB)**
10	<0-72.02	~ -146 – 72.02	<146
20	0-81.12	~ -146 – 81.12	~146
30	0-86.53	< -148 – 86.53	>148
40	0-90.48	< -149 – 90.48	>149
50	0-93.64	< -151-93.64	>151

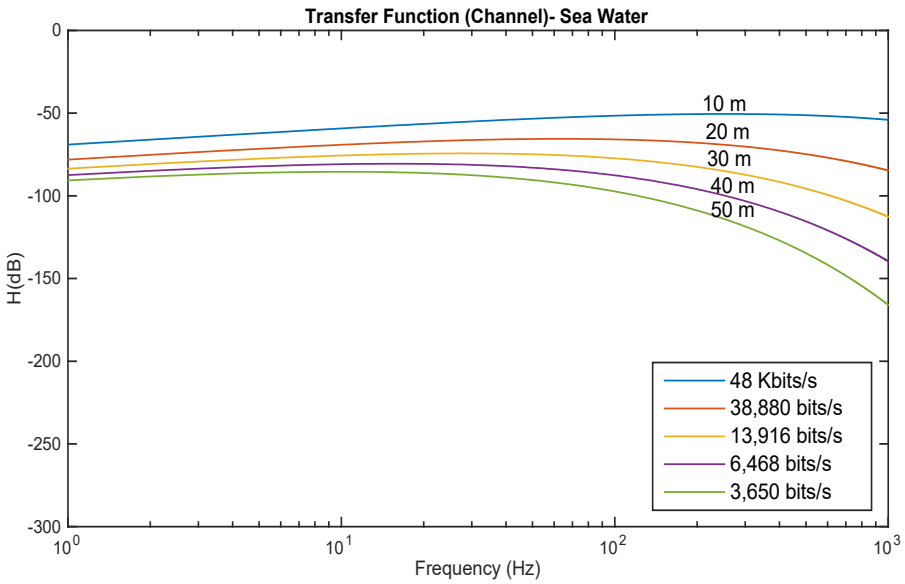

Figure 17 Flat attenuation downlink (SNR)-Seawater (Example1).

Table 10 Flat attenuation downlink (SNR)-Fresh water (Example1).

Communication Range (m)	**S (dB) = P_tx + Channel Attenuation**	**N (dB) Attenuated Atmospheric Noise**	**SNR (dB)**
10	<0-72.01	~ -134-72.01	< 134
20	0-81.04	~ -134-81.04	134
30	0-86.32	~ -136-86.32	136
40	0-90.07	~- 137-90.07	137
50	0-92.98	~ -138-92.98	138

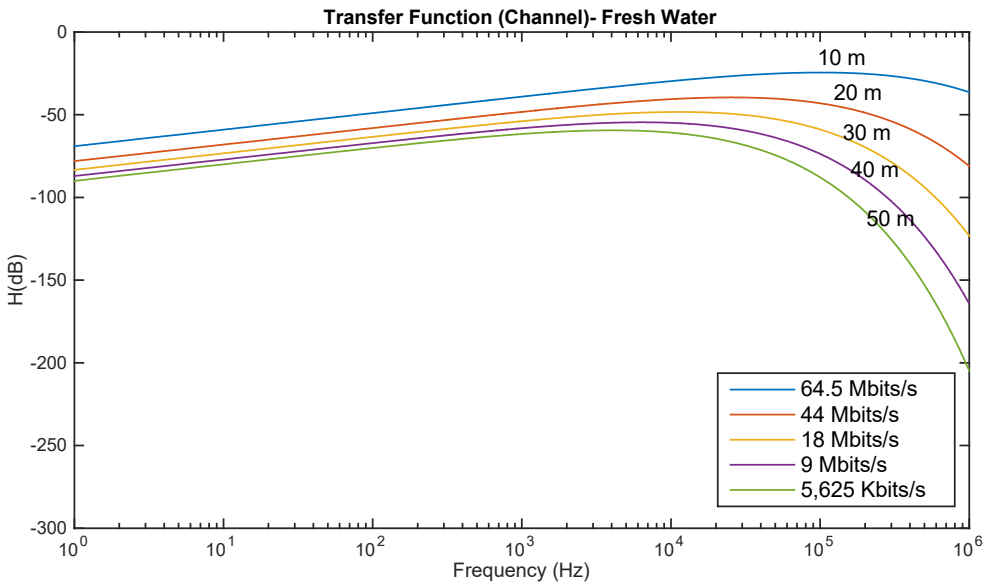

Figure 18 Flat attenuation downlink (SNR)-fresh water (Example1).

In another example (see Figure 19), the communication will consider a submarine at a depth of 50m, with divers submerged between the submarine and water surface. The deployed submarine coil is very large and the diver's coils are quite light and small. The merit factor (here, based on p. 48 of the reference [2]) should be greater than 0.25 so that we can ignore the thermal part of the noise and then $F_a(f)(dB) = 294.15 - 36\log(f)$. Thus, for having a merit factor of at least 0.25, we can choose antennas as detailed below: The specifications of the submarine's antenna are: r=10m, M= 16 Kg, $\sqrt{\sigma/\rho} = 50$, which can give us $\emptyset_s = 1000$. Meanwhile, the specifications of the diver's antenna are: r=0.1m, M= 0.25 Kg, $\sqrt{\sigma/\rho} = 40$, giving us $\emptyset_d = 1$. So $\emptyset = \emptyset_b \times \emptyset_d = 1000$, which is greater than 0.25 and thus all assumptions and approximations are valid.

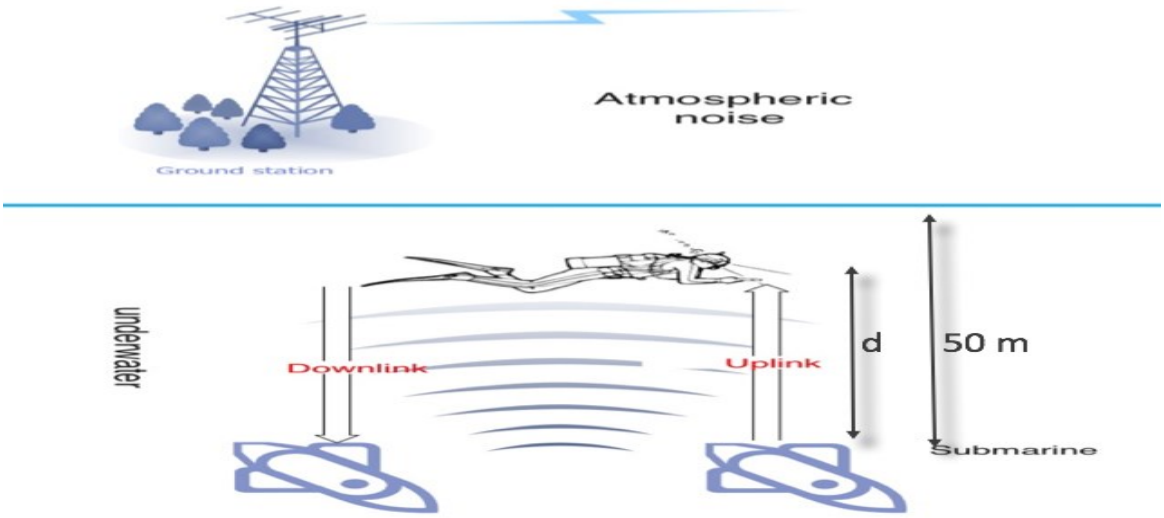

Figure 19 Example 2 for uplink and downlink communication.

The communication range is maximum 50m, and since we are working in near-field and T<<1 (T=0.2 in our MATLAB code), $T = \frac{r}{\delta} << 1$. During our previous simulations, we assumed it as 0.2.

Uplink and Downlink SNR

Based on the topology of the situation, both submarine and diver coils are exposed to attenuated atmospheric noise instead of its full value for both uplink and downlink communications. The transmission power of the submarine and diver coils is 0 dB for initialization, and the channel loss (which consists of cubic distance attenuation combined with exponential absorption loss due to skin depth) is calculated using MATLAB (SkinDepth_Equ_88_V4.m). The results are shown in Tables 12 and 13.

For uplink communication, the diver's coil will receive the atmospheric noise from the atmosphere, which is located above the coil. Thus, the signal travels distance "d" from the

submarine and the atmospheric noise travels from the water surface to the diver's coil "distance of 50-d".

For downlink communications, the signal from the diver's coil to the submarine's coil travels a distance d, while the atmospheric noise travels $50\,m$ from the surface to the submarine location.

Table 11 Flat attenuation uplink and downlink (SNR)-Seawater (Example2).

Communication Range (m)	**S (dB) P_tx + Channel Attenuation**	**N (dB) Attenuated Atmospheric Noise Uplink**	**SNR (dB) Uplink**	**N (dB) Attenuated Atmospheric Noise Downlink**	**SNR (dB) Downlink**
10	<0-72.02	~ -146 -90.48	<164.48	~ -146 -93.64	<167.62
20	0-81.12	~ -146-86.53	~151.41	~ -146-93.64	~158.52
30	0-86.53	< -148-81.12	>142.59	< -148-93.64	>155.11
40	0-90.48	< -149-72.02	>130.54	< -149-93.64	>152.16
50	0-93.64	< -151-93.64	>151	< -151-93.64	>151

Table 12 Flat attenuation uplink and downlink (SNR)-Fresh water (Example2).

Communication Range (m)	**S (dB) P_tx + Channel Attenuation**	**N (dB) Atmospheric Noise Uplink**	**SNR (dB) Uplink**	**N (dB) Atmospheric Noise Downlink**	**SNR (dB) Downlink**
10	<0-72.01	~ -134-90.07	<152.06	~ -134-92.98	<154.97
20	0-81.04	~ -134-86.32	139.28	~ -134-92.98	145.94
30	0-86.32	~ -136-81.04	130.72	~ -136-92.98	142.66
40	0-90.07	~- 137-72.01	118.94	~- 137-92.98	139.91
50	0-92.98	~ -138-92.98	138	~ -138-92.98	138

In the following example, the frequency has been assumed of 30Hz and a sea conductivity of 4 $\mathrm{S/m}$, resulting in a skin depth of $46\mathrm{m}$. The atmospheric noise temperature $\mathrm{F_a} = 241\mathrm{dB}$ (Table 6) results in induced voltage at receiver antenna of 4nV. The Mass of the transmitter antenna weighs 1Kg and has a diameter of 4m. Hence, the dissipating power of 1 w results in a magnetic moment of $100\mathrm{Am}^2$ with a merit factor of $\phi_t = 100\mathrm{Am}^2/\Omega$.

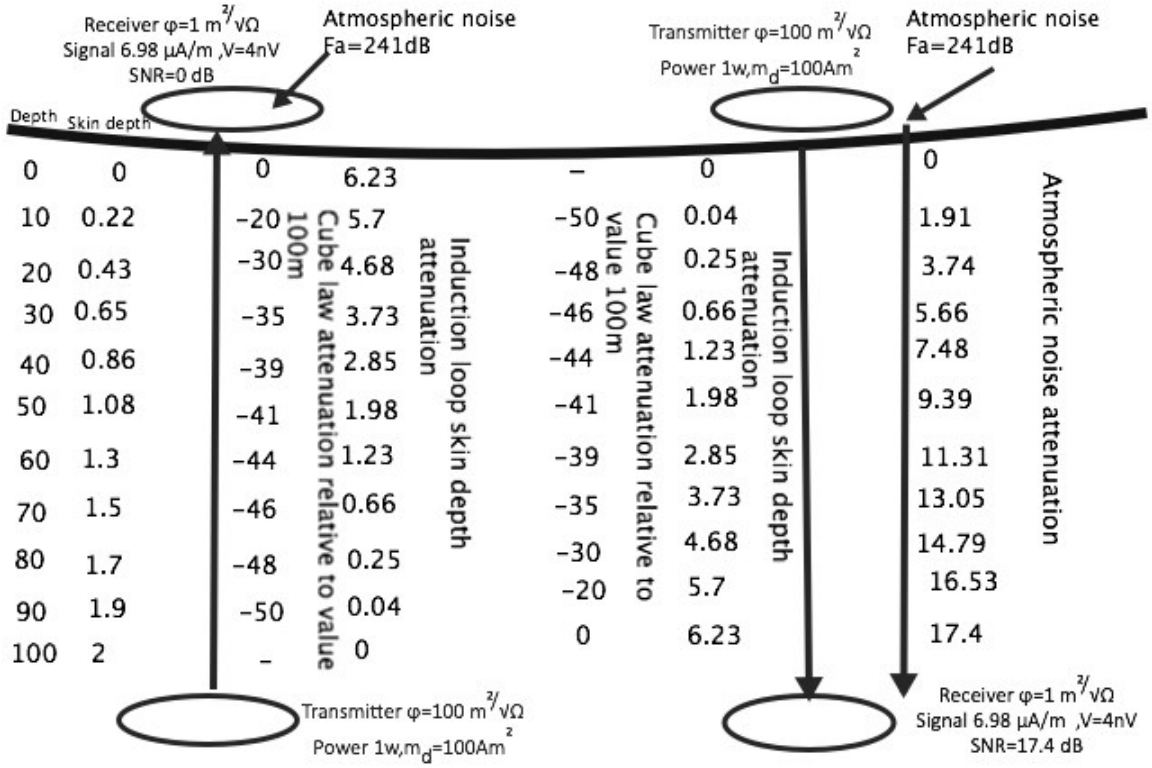

Figure 20 SNR comparison for up-link and downlink operation.

1-Up-link Operation

In viewing Figure 20, which shows the SNR of 0 dB, we can assert that it is a convenient value to describe the sensitivity of an antenna. However, despite its convenience, it is too low to use in operations. Let us assume an operating distance of 50m ($T = 1.08$). The signal strength will be 41 dB due to cube law attenuation and 1.98 dB instead of 6.23 due to induction skin depth attenuation, resulting in SNR of 42.98 dB.

2- Down-link Operation

In downlink operations, the atmospheric noise is attenuated as 8.7 per skin depth. If we are operating at 50m ($T = 1.08$), the SNR at the underwater receiver is increased by 9.39dB due to atmospheric noise attenuation. Thus, we can conclude that we have a SNR of 52.37 dB at a range of 50m. If we want to keep the SNR at 42.98dB of up-link example, the transmitter power must be reduced by 9.39dB or the underwater receiver antenna reduced by 9.39dB (i.e., it must have a merit factor 2.9 times smaller).

CHAPTER5 CONCLUSION

This study examined the feasibility of improving communication under fresh and sea water by way of a magneto-inductive (MI) communication method using a pair of coils as a transmitter and receiver. In modeling the MI channel, both thermal and atmospheric noise were studied and analyzed; however, under some certain circumstances and if the antenna's merit factor were greater than 0.25, the thermal noise could be ignored due to its insignificance against atmospheric noise. The atmospheric noise by itself followed a logarithmic equation that provided an approximate atmospheric noise-temperature ratio.

In terms of the communication field, the near-field region was the only one of interest in the present dissertation. The near-field region covered all field points where the field equations were described by quasi-static field formulas. It was also characterized by the ratio of distance to skin depth, which had to be considerably less than 1. For the current research and during the all MATLAB simulations, it was set to 0.2.

A cubic distance attenuation integrated with an exponential absorption loss was the channel model used for the entire investigation. Its low pass characteristic was verified by MATLAB simulations for both fresh and sea water, showing 0.01 and 4 S/m conductivities. Thus, compared to sea water channel simulation results, fresh water offered a significantly higher bandwidth communication channel. Consequently, better capacity was achievable with the same transmission power. This indicates that the channel attenuation for sea water was notably greater than the signal attenuation over a fresh water communication channel.

For example, to attain a distance of 100m, the channel bandwidth for fresh water was 25 KHz with an attenuation of -102.1 dB, whereas for sea water, these figures were degraded to 10 Hz and -104.5 dB, respectively.

In terms of channel capacity, a better one is attainable for fresh water communication. Thus, for communicating over a distance of 100m, a capacity of roughly 315.51 Kbps was achievable for fresh water communication, whereas exchanging less than 200 bps was possible for a sea water MI communication scheme.

In addition to channel transfer function modeling and its dependency on water conductivity, transmission SNR proved to be another main factor for achieving a certain range of effective communication, bandwidth, and channel capacity. However, it is worth noting that a higher SNR can achieve longer communication distances with better bandwidth and channel capacity. Moreover, the received SNR might be different at each side of the MI communication. In other words, when the receiver antenna is at the water surface, it is exposed to a broad range of atmospheric noise. The atmospheric noise then experiences the channel attenuation for the receiving antenna that is under water. Thus, the receiving antenna on the surface collects an attenuated transmitted signal as well as all the atmospheric noise.

However, the SNR for the receiver antenna immersed in water is different, as it detects the attenuated transmitted signal and atmospheric noise coming from the surface downward towards the antenna cross-section. In the latter case, the received noise power is smaller than the former situation, and if communication parties radiate the same transmission

power, its SNR will be higher. The mentioned situation has been demonstrated here by detailed examples and has also been supported by MATLAB simulations.

Future work will focus on the optimization of the proposed and existing systems. Firstly, Gibson showed that an optimal range does exist and that it features minimum channel attenuation between transmitter and receiver. He also derived the T for triaxial and co-planer coils, which is 2.83 and 3.85, respectively, and recommended using those T values as alternative conditions for near-field MI schemes to achieve better results. Secondly, during the course of existing research, the permittivity is assumed to be constant, whereas the reality is that it is variable as well as frequency-, temperature-, and salinity-dependent. Thus, trying to figure out its dependency and introduce the existing model with derived results might give better results in future investigations. Thirdly, different antenna patterns could be modelled and introduced to existing simulations so that the effects of different shapes and designs could be studied in greater detail. Finally, The MI noise analysis and measurements roughly match up, which means that theoretical equations can be used for noise calculations. However, to obtain more accurate results, pre-amplifier noise could be measured with newer and more precise techniques and then added to noise analysis methods.

BIBLIOGRAPHY

[1] B. Gulbahar and O. B. Akan. A communication theoretical modeling and analysis of underwater magneto-inductive wireless channels. *IEEE Transactions on Wireless Communications 11(9),* pp. 3326-3334. 2012. . DOI: 10.1109/TWC.2012.070912.111943.

[2] C. Schlegel, M. Mallay and C. Touesnard. Atmospheric magnetic noise measurements in urban areas. *IEEE Magnetics Letters 5*pp. 1-4. 2014. . DOI: 10.1109/LMAG.2014.2330337.

[3] A. D. W. Gibson, "**Channel Characterisation and System Design for Sub Surface Communications** ." , University of Leeds, 2003.

[4] J. I. Agbinya. Principles of Inductive Near Field Communications for Internet of Things, River Publishers, Denmark, 2011, ISBN: 978-87-92329-52-3.

[5] J. I. Agbinya and M. Masihpour. Near field magnetic induction communication link budget: Agbinya-masihpour model. Presented at 2010 Fifth International Conference on Broadband and Biomedical Communications. 2010, . DOI: 10.1109/IB2COM.2010.5723604.

[6] J. J. Sojdehei, P. N. Wrathall and D. F. Dinn. Magneto-inductive (MI) communications. Presented at MTS/IEEE Oceans 2001. an Ocean Odyssey. Conference Proceedings (IEEE Cat. no.01CH37295). 2001, . DOI: 10.1109/OCEANS.2001.968775.

[7] L. Erdogan and J. F. Bousquet. Dynamic bandwidth extension of coil for underwater magneto-inductive communication. Presented at 2014 IEEE Antennas and Propagation Society International Symposium (APSURSI). 2014, . DOI: 10.1109/APS.2014.6905114.

[8] M. C. Domingo. Magnetic induction for underwater wireless communication networks. *IEEE Transactions on Antennas and Propagation 60(6),* pp. 2929-2939. 2012. . DOI: 10.1109/TAP.2012.2194670.

[9] S. C. Lin *et al*. Distributed cross-layer protocol design for magnetic induction communication in wireless underground sensor networks. *IEEE Transactions on Wireless Communications 14(7),* pp. 4006-4019. 2015. . DOI: 10.1109/TWC.2015.2415812.

[10] S. Kisseleff, I. F. Akyildiz and W. H. Gerstacker. Throughput of the magnetic induction based wireless underground sensor networks: Key optimization techniques. *IEEE Transactions on Communications 62(12),* pp. 4426-4439. 2014. . DOI: 10.1109/TCOMM.2014.2367030.

[11] Seongwon Han *et al*. Evaluation of underwater optical-acoustic hybrid network. *China Communications 11(5),* pp. 49-59. 2014. . DOI: 10.1109/CC.2014.6880460.

[12] T. E. Abrudan *et al*. Impact of rocks and minerals on underground magneto-inductive communication and localization. *IEEE Access 4*pp. 3999-4010. 2016. . DOI: 10.1109/ACCESS.2016.2597641.

[13] X. Tan, Z. Sun and I. F. Akyildiz. Wireless underground sensor networks: MI-based communication systems for underground applications. *IEEE Antennas and Propagation Magazine 57(4),* pp. 74-87. 2015. . DOI: 10.1109/MAP.2015.2453917.

[14] Z. Sun and I. F. Akyildiz. Magnetic induction communications for wireless underground sensor networks. *IEEE Transactions on Antennas and Propagation 58(7),* pp. 2426-2435. 2010. . DOI: 10.1109/TAP.2010.2048858.